



## Control of the energetic proton flux in the inner radiation belt by artificial means

X. Shao,<sup>1</sup> K. Papadopoulos,<sup>1,2</sup> and A. S. Sharma<sup>1</sup>

Received 14 January 2009; revised 29 April 2009; accepted 14 May 2009; published 15 July 2009.

[1] Earth's inner radiation belt located inside  $L = 2$  is dominated by a relatively stable flux of trapped protons with energy from a few to over 100 MeV. Radiation effects in spacecraft electronics caused by the inner radiation belt protons are the major cause of performance anomalies and lifetime of Low Earth Orbit satellites. For electronic components with large feature size, of the order of a micron, anomalies occur mainly when crossing the South Atlantic Anomaly. However, current and future commercial electronic systems are incorporating components with submicron size features. Such systems cannot function in the presence of the trapped 30–100 MeV protons, as hardening against such high-energy protons is essentially impractical. The paper discusses the basic physics of the interaction of high-energy protons with low-frequency Shear Alfvén Wave (SAW) under conditions prevailing in the radiation belts. Such waves are observed mainly in the outer belt, and it is believed that they are excited by an Alfvén Ion Cyclotron instability driven by anisotropic equatorially trapped energetic protons. The paper derives the bounce and drift-averaged diffusion coefficients and uses them to determine the proton lifetime as a function of the spectrum and amplitude of the volume-averaged SAW resonant with the trapped energetic protons. The theory is applied to the outer and inner radiation belts. It is found that the resonant interaction of observed SAW with nT amplitude in the outer belt results in low flux of trapped protons by restricting their lifetime to periods shorter than days. A similar analysis for the inner radiation belt indicates that broadband SAW in the 1–10 Hz frequency range and average amplitude of 25 pT would reduce the trapped energetic proton flux by more than an order of magnitude within 2 to 3 years. In the absence of naturally occurring SAW waves, such reduction can be achieved by injecting such waves from ground-based transmitters. The analysis indicates that such reduction requires injection of less than 10 kW of SAW power. Increasing the power will result in the further decrease of the trapped flux. The paper concludes with a brief discussion of techniques that can inject such waves using ground-based transmitters.

**Citation:** Shao, X., K. Papadopoulos, and A. S. Sharma (2009), Control of the energetic proton flux in the inner radiation belt by artificial means, *J. Geophys. Res.*, *114*, A07214, doi:10.1029/2009JA014066.

### 1. Introduction

[2] The structure and behavior of the energetic electrons and protons trapped in Earth's Radiation Belt (RB) has been the subject of numerous experimental and theoretical studies [Farley and Walt, 1971; Schulz and Lanzerotti, 1974; Huston and Pfizter, 1998; Selesnick *et al.*, 2007]. Morphologically we can distinguish two regions, the inner RB for  $L$  shells lower than two and the outer RB for  $L$  shells higher than two. The inner RB is dominated by protons with energy in excess of 10 MeV and lifetimes from a few years at low altitudes of 400–500 km [Filz and Holeman, 1965]

to many tens of years at higher altitudes [Selesnick *et al.*, 2007]. Overall the inner belt energetic protons are relatively stable with a typical lifetime of  $\sim 10$  years. Contrary to this the outer RB is very dynamic and dominated by energetic electron fluxes associated with solar events and space weather processes. Inner RB protons are the major cause of performance anomalies and lifetime limitation for Low Earth Orbiting (LEO) satellites. This effect is accentuated by the presence of the South Atlantic Anomaly (SAA), a region where the proton flux is closest to the ground reaching altitudes as low as 200 km. For example, the intolerable frequency of Single Event Upsets (SEU) of the IBM 603 microprocessors (based on  $\sim 0.5$  micron CMOS technology) in Iridium forced Motorola to disable the cache while transiting the SAA.

[3] The main objective of the paper is to develop a comprehensive theory of the interaction of SAW in the ULF frequency range with energetic protons trapped in the radiation belts. The paper is organized as follows: The next

<sup>1</sup>Department of Astronomy, University of Maryland, College Park, Maryland, USA.

<sup>2</sup>Department of Physics, University of Maryland, College Park, Maryland, USA.

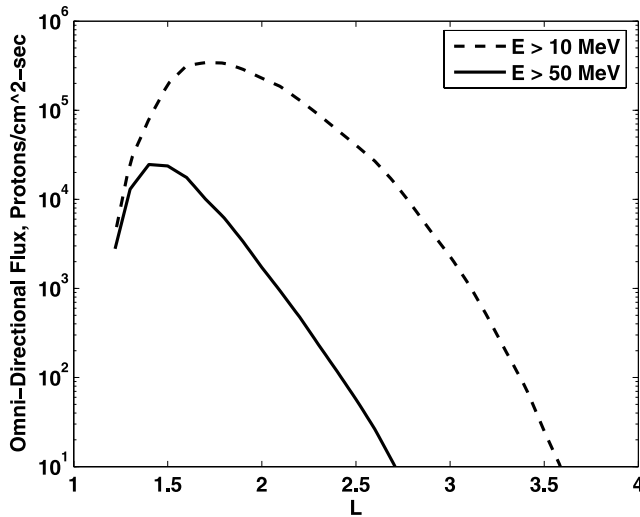


**Figure 1.** Omnidirectional integral proton flux versus  $L$  for energies greater than 10 and 50 MeV (from NASA AP-8 model).

section addresses current thinking on the physics of energetic proton loss rate from the RB. Sections 3–6 discuss the resonant interaction of trapped energetic protons with Shear Alfvén Waves (SAW). In particular, section 3 reviews the basic physics of resonant interaction of protons with SAW and determines the SAW frequency and bandwidth required to interact resonantly with trapped 30–100 MeV protons. Section 4 computes the bounce and drift averaged effective pitch angle diffusion coefficient and the resultant loss rate as a function of the frequency, bandwidth and amplitude of SAW, proton energy and  $L$  shell location. The remaining sections apply the results to the inner and outer RB. Section 5 tests our theoretical formulation against observations and previous theories of proton precipitation in the outer RB. It is found that the presence of SAW with nT amplitude is consistent with lifetimes of the order of days and results in the observed low trapped energetic proton flux for  $L > 2$ , in agreement with earlier estimates [Dragt, 1961]. In section 6, these results are applied to the inner radiation belt. After noting the absence of naturally driven SAW, we examine the possibility and requirements of artificial SAW injection that can lower the inner belt proton fluxes with their associated deleterious consequences on the performance of present and future LEO satellites. The final section addresses briefly some elementary system concepts as well as environmental issues associated with the artificial removal of energetic protons from the inner RB.

## 2. Lifetime of Energetic Protons in the Radiation Belts—Physics Considerations

[4] The source of trapped protons in the inner RB and the physics that controls their loss has been the subject of extensive theoretical and observational papers over the last fifty years [Dragt, 1961, 1971; Farley and Walt, 1971; Schulz and Lanzerotti, 1974; Huston and Pfitzer, 1998; Selesnick et al., 2007]. It is widely recognized that the source and loss mechanisms that control radiation belt

particles are not fully understood [Walt, 1996]. For LEO, 30 MeV protons have lifetimes of  $>20$  years, according to studies based on drift shell tracing [Pu et al., 2005]. On the other hand, at LEO orbits below 500 km, lifetime are less than a few years [Filz and Holeman, 1965]. Theoretical work by Farley and Walt [1971] and Selesnick et al. [2007] suggested that the Cosmic Ray Albedo Neutron Decay (CRAND) is the dominant source of protons with energy  $>100$  MeV or  $L < 1.3$ , and solar energetic protons (SEP) are dominated source for energies  $<100$  MeV and for  $L > 1.3$ . The CRAND source is attributed to radioactive decay of albedo neutrons produced by collisions of energetic cosmic rays with atmospheric nuclei. Both experimental measurements [Filz and Holeman, 1965] following the Starfish detonation and other theoretical and observational evidence [Farley and Walt, 1971; Schulz and Lanzerotti, 1974] indicate that the dominant loss mechanism is proton slowing down by exciting and ionizing ambient Oxygen atoms at low altitude together with significant energy loss to ionize neutral N, He, and H at various altitudes. The loss time due to such a process scales as  $1/\langle\rho\rangle$ , where  $\langle\rho\rangle$  is the atomic electron density averaged over a proton orbit [Cornwall et al., 1965]. In fact, a good fit to the data is that the proton lifetime in the inner RB is given by Dragt et al. [1966]:

$$\tau_L \approx 2 \times 10^4 (E/\text{MeV})^{1.3} (\text{cm}^{-3}/\langle\rho\rangle) \text{ years.} \quad (1)$$

[5] Figure 1 shows the omnidirectional integral proton flux for energies greater than 10 and 50 MeV as a function of the  $L$  value and points out an apparent dilemma in the physics controlling the loss processes in the outer belts, first addressed by Dragt [1961]. The unexpected feature is the sharp gradient in the proton flux between the inner and outer belts. On the basis of the steady state transport equation the ratio of the proton flux  $F(L)$  at  $L = 1.5$  to that of the flux at  $L = 2.5$  will be given by

$$F(L = 1.5)/F(L = 2.5) = [S(L = 1.5)/S(L = 2.5)] \cdot [\tau_L(L = 2.5)/\tau_L(L = 1.5)]. \quad (2)$$

[6] In equation (2)  $S(L)$  and  $\tau_L(L)$  represent the proton source injection rate and lifetime at the particular energy range and  $L$  shell. If we assume that the outer belt lifetime is controlled by the same physics as the inner belt and use equation (1) in conjunction with the density model of Cornwall et al. [1965] we find that the ratio  $\tau_L(2.5)/\tau_L(1.5) \approx 5 \times 10^{-3}$  while from Figure 1 the flux ratio for 50 MeV protons is 200. This implies that either the source  $S(L = 1.5)$  is  $10^4$  times stronger than the  $S(L = 2.5)$ , or that the loss rate at the outer belt is controlled by different physics. However, as noted by Dragt [1961] even if we assume that the CRAND source is the only source at the outer belt, the injection ratio cannot be larger than a factor of 5–10, as expected by geometric attenuation of the flux. Dragt [1961] then proceeded to account for this discrepancy by postulating that while the proton lifetime in the inner RB is dominated by collisional proton slowing down, the proton lifetime in the outer RB is dominated by collisionless physics, such as by pitch angle scattering due to interaction of protons resonating with naturally generated SAW in the Pc1 range. Using equation (2) and  $S(L = 1.5)/S(L = 2.5) \approx 5–10$  we find

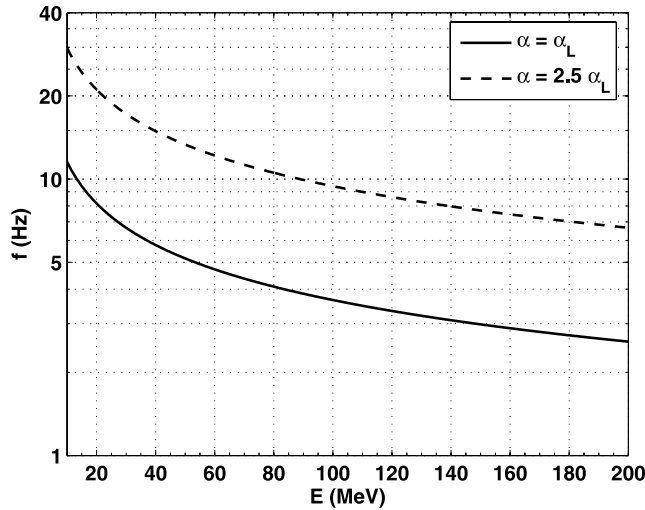


**Figure 2.** The minimum resonant SAW frequency versus proton energy for different pitch angle  $\alpha$  under conditions typical of the magnetic equator of  $L = 1.5$ .

a flux ratio of 200 requires  $\tau_L(L = 2.5)/\tau_L(L = 1.5) \leq 10^{-3}$ . Given that for fluxes above 50 MeV the lifetime near  $L \approx 1.5$  is approximately 20 years the required lifetime due to resonant pitch angle scattering is the range of few hours to days. According to *Dragt* [1961] such lifetime at  $L = 2-2.5$  requires the presence of SAW with frequency in the vicinity of 1 Hz with amplitude  $\sim$  nT. Such waves have been observed in the outer RB and attributed to cyclotron instabilities driven by anisotropic proton distributions. They are also observed on the ground as Pc1 pulsations. Such waves, however, cannot pitch angle scatter 10–100 MeV protons at  $L = 1.5$  in the inner RB.

[7] These observations form the motivation for the inner RB application of this work, as discussed in sections 6 and 7, viz. to study the potential control of the flux level of energetic protons trapped in the inner RB by enhancing the amplitude of SAW by artificial means.

### 3. Resonant Interaction of SAW With Energetic Protons

[8] Inside the magnetosphere SAW propagates mainly along the magnetic field line with frequency much lower than ion cyclotron frequency and is the main source of magnetic field fluctuations. Consider the interaction of SAW with frequency  $\omega$  with an energetic proton. Cyclotron resonance occurs when the Doppler shifted wave frequency seen in the frame of the energetic proton is approximately equal to a harmonic of its gyrofrequency  $\Omega$  as given by the condition

$$\omega - k_z v_z = \frac{\pm n \Omega}{\gamma}. \quad (3)$$

[9] Here  $\omega$  is the wave angular frequency,  $k_z$  is the parallel wave number,  $\gamma = (1 - v^2/c^2)^{-1/2}$ , and  $n = 1, 2, 3, \dots$  are the harmonic resonance numbers. The “+” and “−” signs correspond to normal and anomalous Doppler resonance, respectively. We concentrate here on the primary ( $n = 1$ )

resonance of nonrelativistic protons with left-hand polarized SAW with frequency  $\omega \ll \Omega$ . Under these conditions and using the dispersion relation for SAW

$$\omega = k_z V_A, \quad (4)$$

we find that protons with velocity  $v$  resonate with SAW with frequency  $\omega$  when

$$\omega(v, \alpha) = \frac{\Omega}{\cos \alpha} \frac{V_A}{v}. \quad (5)$$

[10] Here  $V_A$  is the Alfvén velocity and  $\alpha$  is the angle of the proton velocity to the magnetic field (pitch angle). Since we are interested in the SAW-proton interaction outside the loss cone angle  $\alpha_L$  equation (5) defines the minimum frequency required to interact with protons of energy  $E$  as

$$\omega \geq \frac{\Omega}{\cos \alpha_L} \sqrt{\frac{M V_A^2}{2E}}, \quad (6)$$

where  $M$  is the proton mass. Figure 2 shows the minimum resonant frequency as a function of the interacting proton energy for typical equatorial plasma conditions at  $L = 1.5$ . The loss cone angle at  $L = 1.5$  is approximately 28 deg. One can see, for example, that SAW with frequency 13 Hz and bandwidth  $\delta\omega/\omega_0 \approx 1/2$  will resonate with 30 MeV protons at all angles ( $< 2.5 \alpha_L$ ) outside the loss cone, as well as with higher energy trapped protons.

[11] The resonant interaction of the protons with a spectrum of SAW results in pitch angle scattering. The calculation of the resultant diffusion coefficient is well known [Kennel and Petschek, 1966; Steinacker and Miller, 1992; Summers and Thorne, 2003; Albert, 2003]. Assuming a SAW spectrum

$$W(\omega) \propto \exp\left(-(\omega - \omega_0)^2/\delta\omega^2\right), \quad (7)$$

the pitch angle diffusion coefficient is given by

$$D_{\alpha\alpha} \approx \Omega \frac{\delta B(\lambda)^2}{B(\lambda)^2} \frac{\omega(v, \alpha)}{\delta\omega} \exp\left[-(\omega(v, \alpha) - \omega_0)^2/\delta\omega^2\right]. \quad (8)$$

[12] Here  $B(\lambda)$  is the local background magnetic field strength,  $\delta B(\lambda)$  is the amplitude at latitude  $\lambda$ , and  $\omega(v, \alpha)$  is given by equation (5). Notice that the local pitch angle diffusion rate is proportional to the energy of the wave, inversely proportional to the square root of the resonant energy and to the local value of the magnetic field.

[13] In the presence of a monochromatic wave a proton with a specific energy and equatorial pitch angle  $\alpha$  bouncing between two mirroring points satisfies the resonant condition at two conjugate locations. However, in the presence of a broadband spectrum resonance occurs over a range of latitudes. Therefore for broadband waves we solve the gyroresonant condition, equation (5), to obtain the wave frequencies that will resonate with protons of selected energy. The local diffusion rates are then calculated using equation (8) only when the protons are in resonance with waves within the band, defined as  $\omega_0 - \delta\omega < \omega < \omega_0 + \delta\omega$ .

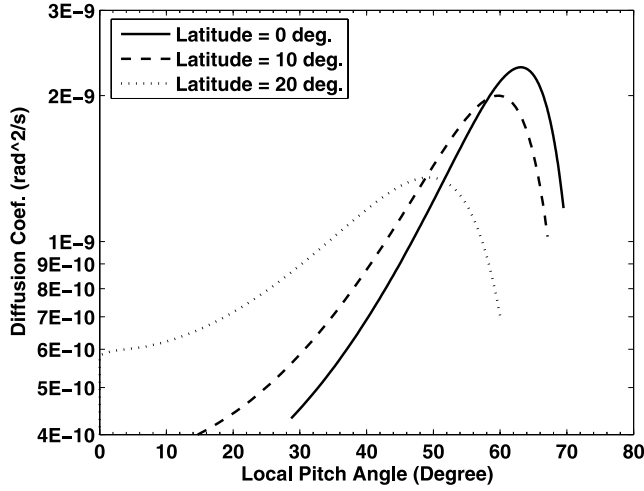


**Figure 3.** The local pitch angle diffusion rates at several locations along  $L = 1.5$  for 30 MeV protons in the presence of waves with frequency 13 Hz and bandwidth 6.5 Hz.

Figure 3 shows the local pitch angle diffusion rate at several locations along the  $L = 1.5$  for 30 MeV energy protons in the presence of waves with frequency 13 Hz bandwidth 6.5 Hz and amplitude 10 pT. It is clear that a relative bandwidth of order unity can scatter energetic protons in a large range of pitch angles. At higher latitudes along the magnetic field, the background magnetic field increases and the overall pitch angle diffusion rate decreases following equation (8), as shown in Figure 3. Figure 3 also shows that the pitch angle scattering range shifts toward lower values and becomes broader at high latitudes. This is due to its dependence on the cosine of resonant pitch angle, viz.  $\cos(\alpha) \propto \Omega V_A$  as described in equation (5). As  $\Omega V_A$  increases by a factor of 1.5 from latitude = 0 deg. to 20 deg., the resonant pitch angle moves to lower values.

#### 4. Computation of Bounce and Drift-Averaged Diffusion and Loss Rates

[14] To obtain the effective pitch angle diffusion of the resonant protons the local pitch angle diffusion coefficient given by equation (8) needs to be integrated over the part of the proton orbit bouncing between the two mirror points. This yields the bounce-averaged pitch angle diffusion coefficient in terms of the particle equatorial pitch angle  $\alpha_E$  and the energy  $E$  as [Lyons and Williams, 1984]:

$$\langle D_{\alpha\alpha} \rangle = \frac{1}{S(\alpha_E) \cos^2(\alpha_E)} \cdot \int_0^{\lambda_M} D_{\alpha\alpha} \sqrt{1 - \sin^2(\alpha_E) B(\lambda)/B(0)} \cos^7(\lambda) d\lambda. \quad (9)$$

[15] Here  $S(\alpha_E) \approx 1.3 - 0.56 \sin \alpha_E$  describes the dependence of the bounce period on the equatorial pitch angle in a dipole magnetic field, and  $\lambda_M$  is the particle mirroring latitude. In equation (9), we assume symmetry with respect to the magnetic equator. We can rewrite the local pitch angle

diffusion rate  $D_{\alpha\alpha}$  (equation (8)) in terms of the latitude  $\lambda$ , particle velocity  $v$  and equatorial pitch angle  $\alpha_E$  as,

$$D_{\alpha\alpha}(\lambda, v, \alpha_E) = \frac{e}{M} \frac{\delta B(\lambda)^2}{B(\lambda)} F(\lambda, v, \alpha_E), \quad (10)$$

where  $F(\lambda, v, \alpha_E) = \frac{\omega(\lambda, v, \alpha_E)}{\delta\omega} \exp[-(\omega(\lambda, v, \alpha_E) - \omega_0)^2/\delta\omega^2]$  and  $\omega(\lambda, v, \alpha_E)$  is given by rewriting the resonant condition (equation (5)) in terms of  $\lambda, v, \alpha_E$  as

$$\omega(\lambda, v, \alpha_E) = \frac{eB(\lambda)}{M} \frac{V_A(\lambda)}{v} \frac{1}{\sqrt{1 - \sin^2(\alpha_E) B(\lambda)/B(0)}}, \quad (11)$$

[16] In deriving equation (11), we have used the conservation of the first adiabatic invariant that relates the particle equatorial pitch angle  $\alpha_E$  to the local pitch angle  $\alpha$  at latitude  $\lambda$  as  $\sin^2 \alpha = \sin^2 \alpha_E B(\lambda)/B(0)$ .

[17] The local wave amplitude  $\delta B(\lambda)$  in equation (10) can be related to the equatorial wave amplitude through the conservation of the wave energy flux and the magnetic flux along the flux tube. This gives

$$\delta B(\lambda)^2 = \delta B(0)^2 \frac{A(0) V_A(0)}{A(\lambda) V_A(\lambda)} = \delta B(0)^2 \frac{B(\lambda)}{B(0)} \frac{V_A(0)}{V_A(\lambda)} = \delta B(0)^2 \sqrt{\frac{\rho(\lambda)}{\rho(0)}}, \quad (12)$$

where  $A(\lambda)$  is the flux tube area, and  $\rho(\lambda)$  is the plasma density at latitude  $\lambda$ . Using equations (10)–(12), the bounce-averaged pitch angle diffusion coefficient (equation (9)) can now be rewritten as

$$\langle D_{\alpha\alpha} \rangle = \frac{e}{M} \frac{\delta B(0)^2}{S(\alpha_E) \cos^2(\alpha_E)} \int_0^{\lambda_M} \frac{1}{B(\lambda)} \sqrt{\frac{\rho(\lambda)}{\rho(0)}} F(\lambda, v, \alpha_E) \cdot \sqrt{1 - \sin^2(\alpha_E) \frac{B(\lambda)}{B(0)}} \cos^7(\lambda) d\lambda. \quad (13)$$

[18] Equation (13) is a key equation of the paper. It gives the average diffusion rate for a proton of energy  $E$ , and equatorial pitch angle  $\alpha_E$ , as a function of the SAW amplitude at the equator and the ratio of  $\rho^{1/2}(\lambda)/B(\lambda) \sim 1/V_A(\lambda)$ . The latter can be taken from models, such as the Global Core Plasma Model (GCPM) [Gallagher et al., 2000]. Before proceeding with the numerical integration of equation (13), we note that the value of  $\delta B(0)^2$  can be related to the average wave energy  $\langle \delta B^2 \rangle / 2\mu_0$  by

$$\frac{\langle \delta B^2 \rangle}{2\mu_0} = \frac{\delta B(0)^2}{2\mu_0} \frac{\int_0^{s_1} V_A(0)/V_A(s) ds}{\int_0^{s_1} B(0)/B(s) ds}, \quad (14)$$

where  $s$  is the distance along the field line, with  $s = 0$  and  $s_1$  defined at the magnetic equator and the reflection point along the field line at altitude  $\sim 110$  km, respectively.

[19] Computation of the equatorial pitch angle distribution and the precipitation lifetime  $\tau_p$  requires solution of the bounce averaged diffusion equation for the proton distribu-

tion function  $f(t, E, L, \alpha_E)$  given by [Lyons and Williams, 1984]:

$$\frac{\partial f}{\partial t} = \frac{1}{S(\alpha_E) \sin(\alpha_E) \cos(\alpha_E)} \frac{\partial}{\partial \alpha_E} \cdot \left[ S(\alpha_E) \sin(\alpha_E) \cos(\alpha_E) \langle D_{\alpha\alpha} \rangle \frac{\partial f}{\partial \alpha_E} \right] - f / \tau_{am}. \quad (15)$$

[20] In equation (15) the loss term is approximated by  $f / \tau_{am}$  and  $\tau_{am}$  equals to half of the bounce period for  $\alpha_E$  within the loss cone and goes to  $\infty$  for  $\alpha_E$  outside the loss cone.

[21] In the absence of a proton source the distribution function will decay to a lowest normal mode of the system whose profile will remain invariant with time [Lyons and Williams, 1984]. The distribution function can then be split into the product of a temporal decay component  $F(t, E, L)$ , and a steady state pitch angle distribution  $g(E, L, \alpha_E)$ . Solving for the temporal decay yields [Abel and Thorne, 1998]

$$\frac{1}{F} \frac{\partial F}{\partial t} = -\frac{1}{\tau_p}, \quad (16)$$

where  $\tau_p$  is the eigenvalue that corresponds to the precipitation lifetime. Using equations (15) and (16) we find

$$\left( \frac{1}{\tau_{am}} + \frac{1}{F} \frac{\partial F}{\partial t} \right) S(\alpha_E) \sin(\alpha_E) \cos(\alpha_E) g(E, L, \alpha_E) = \frac{\partial}{\partial \alpha_E} \left[ S(\alpha_E) \sin(\alpha_E) \cos(\alpha_E) \langle D_{\alpha\alpha} \rangle \frac{\partial g(E, L, \alpha_E)}{\partial \alpha_E} \right]. \quad (17)$$

[22] Given the bounce-averaged pitch angle diffusion rate  $\langle D_{\alpha\alpha} \rangle$  for a proton with energy  $E$  as a function of equatorial pitch angle  $\alpha_E$ , we can apply a finite difference scheme to the right hand side of equation (17) to approximate the derivatives. The steady state distribution function  $g(E, L, \alpha_E)$  is discretized as  $g(E, L, \alpha_{E,i})$ , where  $\alpha_{E,i}$  with  $i = 1, 2, 3, \dots$  are discrete equatorial pitch angles. The discretized equation (17) forms a matrix equation, yielding a nonlinear eigenvalue problem whose solutions, i.e., eigen-vector  $g(E, L, \alpha_{E,i})$  and eigen value  $\tau_p$ , can be obtained by using an iterative method.

[23] Equations (13), (14), (16), and (17) form the key results on which the feasibility and energy and power estimates for the reduction of proton flux is based. These equations need to be integrated numerically by considering a particular value of  $L$  and proton energy, a SAW amplitude, frequency and bandwidth, and a model for the magnetic field and plasma density. This forms the subject of the following sections.

## 5. Outer Radiation Belt Application—Energetic Proton Flux Estimate at the Outer Belt

[24] Alfvén waves are a ubiquitous feature of the outer RB. SAW excitation is attributed to cyclotron instabilities driven by anisotropic proton distributions and the SAW amplitude can be largely enhanced during magnetic storms. Typical SAW wave amplitude in the outer belt is around several nT and can be larger during magnetic storms.

Observations have shown large amplitude waves over a wide range of frequencies. For example, CRRES ( $L = 4.8 - 6.7$ ) detected waves in the Pc1 range with transverse magnetic field perturbations with 3–14 nT peak to peak amplitudes [Fraser et al., 1996]. Viking observations showed magnetic field perturbations with mixed left-hand and right-hand polarizations propagating primarily along the ambient magnetic field [Erlandson et al., 1990]. At lower altitudes, Magsat (350 by 550 km near-polar orbit) measured Pc 1 waves with mixed polarizations with amplitudes of 5–30 nT [Iyemori and Hayashi, 1989]. Such observations show that the presence of SAW and associated waves is atypical feature of radiation belts. Such waves, however, can only propagate across magnetic field lines as compressional mode waves and reach inner belt if they have a frequency below ion cyclotron frequency [Astrom, 1950]. The proton cyclotron frequency at  $L = 5$  is approximately 4 Hz. Therefore the SAWs reaching  $L = 2.5$  from outer belt have a cutoff around 4–5 Hz. We assume that the SAW at  $L = 2.5$  have a broadband spectrum similar to equation (7) with the center frequency near zero with 4 Hz bandwidth. To calculate the local, bounce-averaged diffusion rate and the lifetime for protons, we assume the volume-averaged wave amplitude  $\langle \delta B \rangle$  to be  $\sim 1$  nT at  $L = 2.5$ , which is a fraction of outer belt SAW amplitude.

[25] Figure 4a shows the bounce-averaged pitch angle diffusion rate for 10 and 50 MeV protons at  $L = 2.5$  calculated with equations (8) and (13). The broadband wave with bandwidth = 4 Hz can effectively pitch angle scatter protons with pitch angle upto  $\sim 80$  deg. At  $L = 2.5$ , the loss cone angle is approximately 11.6 deg. We further solve the eigenvalue equation (17) with the bounce-averaged diffusion rate given in Figure 4a. Figure 4b shows the steady state distribution function  $g(E, L, \alpha_E)$  for 10 and 50 MeV protons at  $L = 2.5$ . The resultant lifetimes for 10 and 50 MeV protons are 1 and 1.9 days, respectively. In Dragt [1961], with SAW wave amplitude  $\sim 3$  nT, the lifetime of 100 MeV protons is estimated to be  $\sim 0.5$  day. Our estimation of natural lifetime for 10 and 50 MeV protons using diffusion calculation yields similar life time  $\sim$  days given 1 nT SAW amplitude. Thus the short lifetime of  $>10$  MeV protons at  $L = 2.5$  can be attributed to the pitch angle scattering of protons by SAW.

## 6. Inner Radiation Belt Application—Proton Radiation Belt Remediation (PRBR)

[26] As noted earlier the inner RB is populated by high flux of energetic protons that impact the operation and lifetime of LEO satellites. While currently most of the operational problems are centered in the vicinity of SAA this is not the case for future LEO satellites. High volume production and its associated cost savings force satellite systems to utilize Commercial-Off-the-Shelf (COTS) electronics. The anomalies caused by the impact of energetic protons are known as Single Event Effects (SEE). The SEE anomaly cross section is a strong nonlinear function of the device feature size. Current estimates indicate [Amusan et al., 2007; DasGupta et al., 2007] that SEE cross section increases by a factor of over one hundred in moving from micron scale size to the currently available COTS of 65 nm.

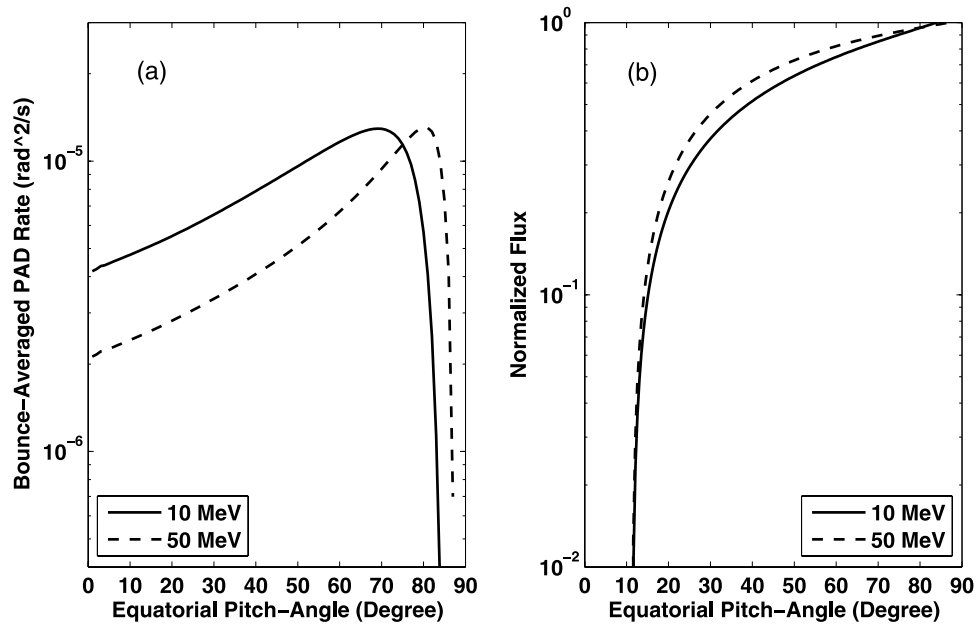


**Figure 4.** (a) The bounce-averaged diffusion rates for 10 and 50 MeV protons at  $L = 2.5$  due to scattering by broadband SAW with center frequency = 0 Hz and bandwidth 4 Hz. The volume-averaged wave amplitude  $\langle \delta B \rangle$  is assumed to be  $\sim 1$  nT. (b) Corresponding steady state distribution function  $g(E, L, \alpha_E)$  for 10 and 50 MeV protons at  $L = 2.5$ .

This implies that in the near future the LEO orbit range for satellites with COTS will be operationally unavailable.

[27] The previous physics analysis on the effect of SAW on proton lifetime, combined with the discussion given in section 2 on the reasons for the sharp trapped proton flux gradient in transitioning from the inner to the outer RB provides a solution to the this dilemma. Namely use ground ULF transmitters to inject into the inner RB SAW with the average energy density required to reduce the proton flux by one or more order of magnitude. Given the long replenishment timescales such reduction can be accomplished slowly, in timescales of two to three years.

[28] At this point we should remark that controlled, enhanced precipitation of relativistic electrons in the slot region of the RB by injecting whistler waves from space platforms is a very active research topic known as RB Remediation (RBR). RBR refers to enhanced precipitation of relativistic electrons injected by the beta-decay of radioactive products following a deliberate or accidental High Altitude Nuclear Explosion [Parmentola, 2001; Papadopoulos, 2001; Steer, 2002; Dupont, 2004]. Such an explosion could increase the relativistic electron flux in the “gap” by more than four orders of magnitude with natural decay rate of several years. This will have catastrophic implications to LEO satellites within a period of one week. RBR aims at injecting sufficient VLF power in the gap region to reduce the lifetime to less than a few days. Ganguli *et al.* [2006] have discussed VLF wave injection by taking advantage of the free energy available by the release of few tons of Ba from a rocket at 500 km altitude. Such a release could create whistler waves with extremely high amplitude capable of achieving lifetime of less than an hour. An alternative pursued is injection of whistler waves from a constellation of space-based transmitters [Inan *et al.*, 2003]. Besides the physics considerations that differentiate the RBR to the

proton control scheme discussed here, an important difference is on the decay timescale. Following the RBR nomenclature we refer to the proton reduction scheme discussed here as Proton Radiation Belt Remediation (PRBR) Notice that while RBR requires fast action on the order of hours to days, PRBR involves slow and controlled action and with timescale of years.

### 6.1. PRBR Frequency and SAW Amplitude Requirements

[29] Figures 5a–5c show examples of the bounce-averaged pitch angle diffusion rate at  $L = 1.5$  for energetic protons in the presence of three different broadband SAW calculated using equation (13). The center frequency of the SAW used in the examples were chosen to effectively scatter protons with pitch angle  $\alpha_L < \alpha_E < 2.5\alpha_L$  and energy 100, 50 and 30 MeV most efficiently, as seen in Figure 2. The bandwidths were taken as half of the central frequencies. In calculating the bounce-averaged pitch angle diffusion rate, a volume-averaged wave amplitude  $\langle \delta B \rangle \sim 25$  pT was assumed. The diffusion rate scales as the square of the amplitude. Table 1 lists the loss times for multienergy protons calculated by solving equation (17) and using the bounce-averaged pitch angle diffusion rates obtained in Figures 5a–5c. Figures 5d–5f show the corresponding steady state distribution function  $g(E, L, \alpha_E)$  for three protons energies at  $L = 1.5$  due to scattering by broadband SAW with spectrum given in Figures 5a–5c, respectively.

[30] In solving equation (17) to obtain the proton lifetimes, we used a loss cone angle of  $\alpha_L = 28$  deg., which corresponds to the protons lost at altitude 110 km along  $L = 1.5$ . The lifetime of protons at altitudes below 400–500 km can be less than few years [Filz and Holeman, 1965] and thus is comparable to the remediation timescale. This implies that for the wave power being considered the

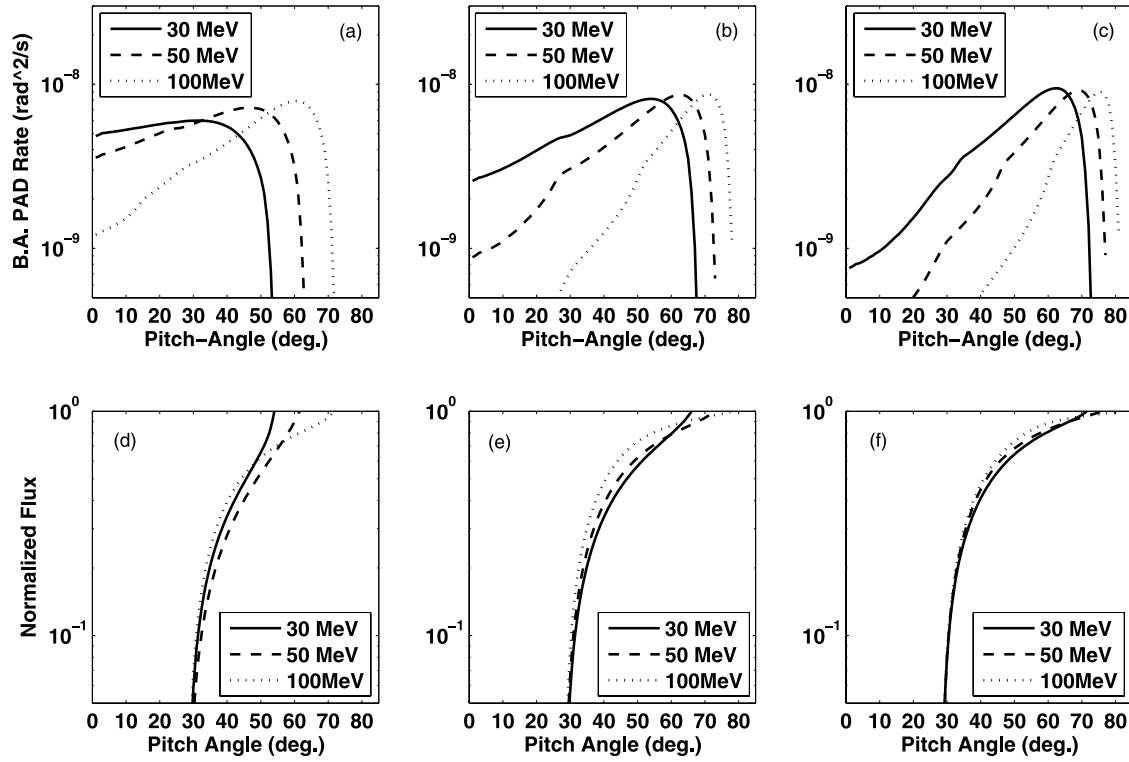


**Figure 5.** (top) The bounce-averaged diffusion rates for three protons energies at  $L = 1.5$  due to scattering by broadband SAW with center frequency of (a)  $f_1 = 6.5$  Hz, (b)  $f_2 = 10$  Hz, and (c)  $f_3 = 13$  Hz. The bandwidths of these broadband waves are half of the center frequencies. The volume-averaged wave amplitude  $\langle \delta B \rangle$  is assumed to be  $\sim 25$  pT. (bottom) Corresponding steady state distribution function  $g(E, L, \alpha_E)$  for three protons energies at  $L = 1.5$  due to scattering by broadband SAW with spectrum given in Figures 5a–5c.

remediation will substantially decrease proton intensity at altitudes ( $>400$ – $500$  km), while its effects at low altitudes will be diminished.

[31] From Figure 5, we see that broadband SAW can pitch angle scatter protons with different energies and the effective pitch angle range for scattering varies with wave spectrum. With lower frequency, i.e.,  $f_1 = 6.5$  Hz, the loss time for 100 MeV protons can be reduced to  $\sim 1.6$  years. However, this SAW spectrum can scatter effectively only the protons with lower energies and narrower pitch angle range, e.g.,  $\alpha_E < 52$  deg. for 30 MeV protons. The loss time for 30 MeV protons is around 4.6 years. On the other hand, with higher frequency, i.e.,  $f_3 = 13$  Hz, the pitch angle range for scattering can cover  $\alpha_L < \alpha_E < 2.5\alpha_L$  for 30–100 MeV protons. Using this broadband spectrum of  $f_3 = 13$  Hz, the loss time of 30–50 MeV protons can be 2.5 years and the loss time of 100 MeV protons is around 4 years. Taking into account of these tradeoffs, a broadband SAW with center frequency  $f_2 = 10$  Hz and bandwidth of 5 Hz can be optimum. It can reduce the loss time of 30–100 MeV protons to be within 3 years and most effectively reduce the loss time of 50 MeV proton to 1.6 years. Clearly these results should be taken as simple guides as to the selection of the parameters of an operating system.

## 6.2. SAW Injection Power Requirements

[32] To estimate the SAW injection power required to achieve a loss time of,  $\sim 2$ – $3$  years we use the parameters discussed in the previous section, namely  $\langle \delta B \rangle \approx 25$  pT. For

definiteness consider a volume contained between a shell of dipole field lines at  $L = 1.5$  with width  $\delta L \approx .1$ . Since the volume is approximately  $\delta V \approx 3 \times 10^{20}$  m<sup>3</sup> the required steady state energy of the waves is given by  $W \approx ((\delta B)^2 / 2\mu_0) \delta V = 75$  kJ.

[33] To find the power required to maintain such an average energy we consider the shell as a leaky cavity whose boundaries at the ionospheric boundaries have a reflection coefficient  $R = \frac{\sum_P - \sum_A}{\sum_P + \sum_A}$ , where  $\sum_P$  is the height-integrated Pedersen conductivity and  $\sum_A = 1/Z_A$  where  $Z_A$  is the Alfvén wave impedance. The evolution of wave energy trapped inside the leaky cavity can be written as

$$\frac{dW}{dt} = P - \nu W, \quad (18)$$

where  $W$  is the wave energy,  $P$  is the wave energy injection rate and  $\nu$  is the energy loss rate. The energy loss rate due to

**Table 1.** Loss Time of Protons of Different Energies at  $L = 1.5$  Due to Pitch Angle Scattering by Alfvén Waves With Various Spectrums Used in Figure 5

	$f_1 = 6.5$ Hz	$f_2 = 10$ Hz	$f_3 = 13$ Hz
$E = 30$ MeV	1688 days	880 days	595 days
$E = 50$ MeV	900 days	586 days	920 days
$E = 100$ MeV	580 days	1032 days	1600 days

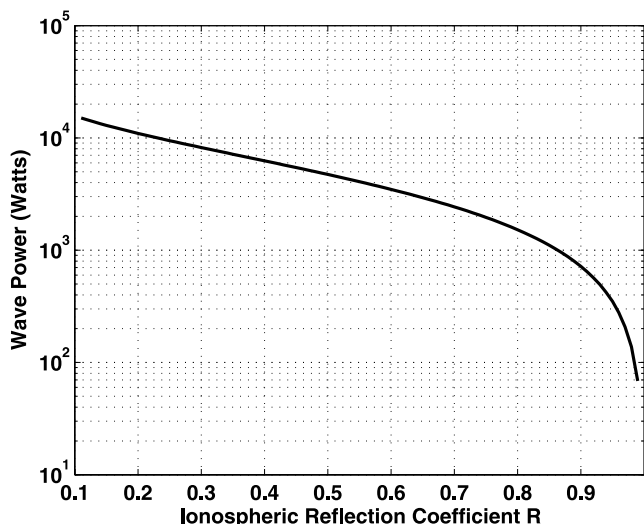


**Figure 6.** Dependence of injected wave power on ionospheric reflection coefficient  $R$  to maintain wave energy  $W = 75$  kJ inside the shell volume at  $L = 1.5$  with  $\delta L = 0.1$ , assuming a wave transit time of 11 sec.

transmission at the ionospheric boundary is  $\nu = -\ln R/\Delta T$ , where  $R$  is the reflection coefficient at the ionospheric boundary and  $\Delta T$  is the Alfvén wave propagation time along the magnetic field line. In steady state the power  $P$  required to maintain SAW energy  $W$  is given by

$$P = \nu W = -\frac{\ln R}{\Delta T} W. \tag{19}$$

[34] Figure 6 shows the input power required to maintain a wave energy of 75 kJ, assuming a wave transit time of 11

sec, as a function of the ionospheric reflection coefficient  $R$ . For example, to maintain wave energy  $W = 75$  kJ inside the shell volume at  $L = 1.5$  with  $\delta L = 0.1$ , we should inject  $P \sim 700$  W for  $R = 0.9$ , and  $P \sim 3500$  W for  $R = 0.6$ . The resultant proton loss time will be approximately 3 years. The loss time scales linearly with the injected SAW power.

### 6.3. Elementary System Concepts and Environmental Issues

[35] The paper presents an analysis of the interaction of artificially generated SAW injected in the inner RB with trapped energetic protons in the 30–100 MeV range. The results indicate that injection of few kW of SAW power in the 1–10 Hz frequency range in the inner radiation belt can result in significant reduction of the proton flux on time-scales of few years. The analysis should be considered as a first order guide to spark a combined research and engineering study as to the viability of such a system. Although this is not the subject of the present study we feel compelled to mention a number of options for transmitter systems and locations.

[36] From the practical power and engineering point of view a ground based ULF transmission system is clearly preferred over a space based system. Such a system can be located at the foot of the particular field line or distributed in a range of appropriate azimuths. For a ground based transmitter we examine two options. The first is a traditional Horizontal Electric Dipole (HED) such as the Michigan system that was used for communications with submarines. *Greifinger and Greifinger* [1974] in fact examined the possibility to use such a HED antenna to inject magnetosonic waves in the Alfvénic waveguide at Pc1 frequencies for lateral propagation studies. The power injected into magnetosphere by an HED can be estimated by referring to Figure 7a. The magnetic and electric fields at the base of

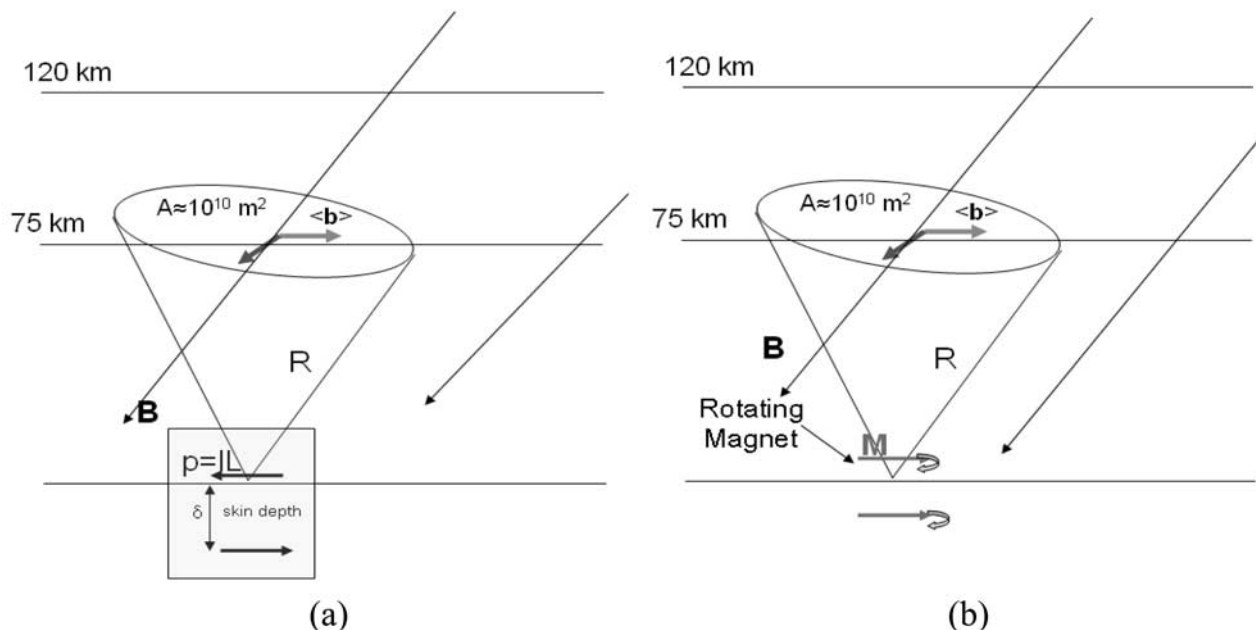


**Figure 7.** Schematic illustration of SAW injected into the ionosphere using (a) Horizontal Electric Dipole (HED) and (b) Horizontal Magnetic Dipole (HMD) antennas.

the ionosphere, taken to be at an altitude of 75 km where the electrons become magnetized, will be given by

$$H_y \approx \frac{IL}{4\pi h^2}(\delta/h), \quad E_x \approx Z(h) \frac{IL}{4\pi h^2}(\delta/h), \quad (20)$$

$$Z(h) = \sqrt{\frac{i\omega\mu}{\sigma_P(h) + i\omega\varepsilon}}. \quad (21)$$

[37]  $Z(h)$  is the impedance at the bottom of the ionosphere and  $\sigma_P(h)$  is the corresponding Pedersen conductivity. Notice that these are the fields driven by two antiparallel currents (the antenna current and image current) separated by the skin depth distance  $\delta$  and we assumed that  $\delta \ll L$ . From equations (20)–(21) the power density injected in the ionosphere by a HED with dipole moment  $IL$  at a frequency  $f$  is thus given by

$$S = Z_0 \left(1/\sqrt{1 + \sigma_P(h)/i\omega\varepsilon}\right) (IL/4\pi h^2)^2 (\delta/h)^2, \quad (22)$$

where  $Z_0 = 120\pi$  is the impedance of free space. Taking the approximate area at an altitude  $h$  as  $h^2$  we find that in practical units the injected power in the RB will be given by

$$P(z = h) \approx \alpha 4 (IL/3 \times 10^4 A - \text{km})^2 (75 \text{ km}/h)^4 (\delta/7 \text{ km})^2 \text{ kW}. \quad (23)$$

[38] In equation (23)  $\alpha \approx \cos^2 \theta \sqrt{\varepsilon\omega/\sigma_P(h)}$  is the efficiency with which the power at the bottom of the ionosphere will couple to the SAW if the angle that Earth's magnetic field makes to the ground at the transmitter location is  $\theta$ . The injection efficiency along with other design issues will be addressed in detail in a future publication. We simply state here that since the ionospheric attenuation at few Hz frequencies is negligible and using nighttime conditions the factor  $\alpha$  is of order unity. As a zero order estimate a HED with  $L \approx 10$ – $15$  km and  $I \approx 1$ – $3$  kA located on ground with conductivity approximately  $10^{-4}$  S/m could in principle inject a few kW of power into the SAW mode.

[39] An alternative technique for SAW injection utilizes an array of superconducting coils with magnetic moment parallel to the ground and rotating at the relevant frequency  $\omega$ , as shown in Figure 7b. Notice that contrary to the HED, the image source of a rotating Horizontal Magnetic Dipole (HMD) is in the same direction, thereby doubling the strength of the source. The magnetic and electric fields at the bottom of the ionosphere of such a Rotating Magnetic Field (RMF) source will be given approximately by

$$\begin{aligned} \vec{H}(z \approx h) &\approx \frac{M(\hat{e}_x \cos \omega t + \hat{e}_y \sin \omega t)}{\pi h^3}, \\ \vec{E}(z = h) &\approx Z(h) \frac{M(\hat{e}_y \cos \omega t + \hat{e}_x \sin \omega t)}{\pi h^3}. \end{aligned} \quad (24)$$

[40] In practical units the power injected in SAW will be approximately

$$P \approx \alpha 64 (75 \text{ km}/h)^4 (M/2 \times 10^4 A - \text{km}^2)^2 \text{ kW} \quad (25)$$

[41] An advantage of the RMF system is its compactness and portability. For example, a superconducting magnet with  $25 \text{ m}^2$  area, 400 Amps DC current and  $10^5$  turns has an approximate magnetic moment of  $10^9 \text{ A m}^2$ . Approximately 20 coils will be needed to inject kW level power.

[42] Before closing we remark briefly on potential environmental concerns. We are guided to a great extent by similar considerations addressed in developing the RBR system [Rodger *et al.*, 2006] and an unpublished analysis of a committee appointed by DARPA to examine the potential environmental implications of a PRBR system. The two relevant environmental issues are:

[43] 1. Can the precipitated proton flux change thermospheric composition of minority species, or cause blackout or interruption of transionospheric communications and navigation signals?

[44] 2. What is the effect on Earth's magnetic field of removing a large fraction of trapped particles?

[45] To answer the first question we estimate first the total number of inner belt ( $>10 \text{ MeV}$ ) protons as

$$N = \int_{E=30 \text{ MeV}}^{100 \text{ MeV}} \int_{L=1.2}^2 f_{\text{omni}}(L, E) \frac{\tau_B(L, E)}{2} 2\pi L dL R_E^2 dE, \quad (26)$$

where  $f_{\text{omni}}(L, E)$  is the omnidirectional differential flux for proton of energy  $E$  at location  $L$ . Using the omnidirectional differential proton flux obtained from NASA AP-8 model, we estimate that the total number of 30–100 MeV protons calculated for  $L = 1.2$  to  $2.0$  is  $N(E = 10$ – $100 \text{ MeV}, L = 1.2$ – $2.0) \sim 10^{23}$ . If these protons are removed in one year, the precipitation rate is  $<1/(\text{cm}^2 \text{ sec})$  for a  $\sim 10^6 \text{ km}^2$  foot area in the ionosphere into which protons between  $L = 1.2$  and  $2$  will be precipitated. The background noise in the proton flux is  $10/(\text{cm}^2 \text{ sec})$  and the flux of  $>10 \text{ MeV}$  protons during a solar proton event (SPE) at high latitudes is  $>10^4/(\text{cm}^2 \text{ sec})$  [Verronen *et al.*, 2005; Rodger *et al.*, 2006]. Thus the energetic proton flux arising from PRBR would be less than the background level and at least four orders of magnitude less than natural SPE fluxes. Studies of enhanced radiation during intense solar proton events [Jackman *et al.*, 1995; Verronen *et al.*, 2005] and a high altitude nuclear explosion [Rodger *et al.*, 2006] conclude that these events cause no significant change in the ozone chemistry and RF communications. Thus the effects of the proton fluxes from the proposed remediation are estimated to be minimal to nonexistent.

[46] It is simpler to answer the second question. The plasma is diamagnetic and removing drifting particles will simply increase the value of the ambient magnetic field. In this respect the effect is beneficial in terms of protection from cosmic rays or other charged particle input. However, the magnitude of the diamagnetic effect is extremely small as seen by a simple calculation. The diamagnetic current

due to the energetic inner belt protons can be estimated as [Parks, 2004]

$$I = 3E / (2\pi r^2 B), \quad (27)$$

where  $E$  is the total energy of protons and  $B$  is the local magnetic field. The total energy of the inner belt energetic protons is estimated to be  $8 \times 10^{11}$  Joule by approximating the total number of protons as  $\sim 10^{23}$  and the average proton energy  $\sim 50$  MeV. Therefore equation (27) yields total inner belt proton current  $I \approx 5.8 \times 10^2$  A, where we have taken  $r = 2R_E$ . The magnetic moments of the inner belt proton current is  $M = I \pi r^2 = 3 \times 10^{17}$   $\text{Tm}^3$ , which is four orders of magnitude less than Earth's magnetic moment ( $6 \times 10^{21}$   $\text{Tm}^3$ ).

[47] **Acknowledgments.** ONR MURI grant N00140710789. We thank T. Wallace of BAE Systems-AT and A. Demekhov of Institute of Applied Physics, Russian Academy of Sciences for the important discussions and input and D. Gallagher for providing the Global Core Plasma Model (GCPM).

[48] Zuyin Pu thanks Richard Selesnick for his assistance in evaluating this paper.

## References

- Abel, B., and R. M. Thorne (1998), Electron scattering loss in Earth's inner magnetosphere: 1. Dominant physical processes, *J. Geophys. Res.*, *103*(A2), 2385–2396.
- Albert, J. M. (2003), Evaluation of quasi-linear diffusion coefficients for EMIC waves in a multispecies plasma, *J. Geophys. Res.*, *103*(A6), 1249, doi:10.1029/2002JA009792.
- Amusan, O. A., L. W. Massengill, M. P. Baze, B. L. Bhuvu, A. F. Witulski, S. DasGupta, A. L. Sternberg, P. R. Fleming, C. C. Heath, and M. L. Alles (2007), Directional sensitivity of single event upsets in 90 nm CMOS due to charge sharing, *IEEE Trans. Nucl. Sci.*, *54*(6), 2584.
- Astrom, E. (1950), On waves in an ionized gas, *Arkiv Fysik*, *2*, 443–457.
- Cornwall, J., A. Sims, and R. White (1965), Atmospheric density experienced by radiation belt protons, *J. Geophys. Res.*, *70*(13), 3099–3111.
- DasGupta, S., A. F. Witulski, B. L. Bhuvu, M. L. Alles, R. A. Reed, O. A. Amusan, J. R. Ahlbin, R. D. Schrimpf, and L. W. Massengill (2007), Effect of well and substrate potential modulation on single event pulse shape in deep submicron CMOS, *IEEE Trans. Nucl. Sci.*, *54*(6), 2407.
- Dragt, A. J. (1961), Effect of hydromagnetic waves on the lifetime of Van Allen radiation protons, *J. Geophys. Res.*, *66*, 1641–1649.
- Dragt, A. J. (1971), Solar cycle modulation of the radiation belt proton flux, *J. Geophys. Res.*, *76*(10), 2313–2344.
- Dragt, A. J., M. M. Austin, and R. S. White (1966), Cosmic ray and solar proton albedo neutron decay injection, *J. Geophys. Res.*, *71*(5), 1293–1304.
- Dupont, D. G. (2004), Nuclear explosions in orbit, *Sci. Am.*, *290*(6), 100.
- Erlanson, R. E., L. J. Zanetti, T. A. Potemra, L. P. Block, and G. Homgren (1990), Viking magnetic and electric field observation of Pc 1 waves at high latitudes, *J. Geophys. Res.*, *95*(A5), 5941–5955.
- Farley, T. A., and M. Walt (1971), Source and loss processes of protons of the inner radiation belt, *J. Geophys. Res.*, *76*(34), 8223–8240.
- Filz, R., and E. Holeman (1965), Time and altitude dependence of 55-MeV trapped protons, August 1961 to June 1964, *J. Geophys. Res.*, *70*(23), 5807–5822.
- Fraser, B. J., H. J. Singer, W. J. Hughes, J. Wygant, R. R. Anderson, and Y. D. Hu (1996), CRRES Poynting vector observations of EMIC waves near the plasmopause, *J. Geophys. Res.*, *101*(A7), 15,333–15,343.
- Gallagher, D. L., P. D. Craven, and R. H. Comfort (2000), Global core plasma model, *J. Geophys. Res.*, *105*(A8), 18,819–18,833.
- Ganguli, G. I., M. Lampe, W. E. Amatucci, and A. V. Streltsov (2006), Active Control of Nuclear-Enhanced Radiation Belt, NRL review, pp. 198–201. (Available at [http://www.nrl.navy.mil/Review06/images/06Simulation\(Ganguli\).pdf](http://www.nrl.navy.mil/Review06/images/06Simulation(Ganguli).pdf))
- Greifinger, C., and P. Greifinger (1974), Generation of ULF by a horizontal electric dipole, *Radio Sci.*, *9*(5), 533–539.
- Huston, S. L., and K. A. Pfitzer (1998), A new model for the low altitude trapped proton environment, *IEEE Trans. Nucl. Sci.*, *45*, 2972, doi:10.1109/23.736554.
- Inan, U. S., T. F. Bell, J. Bortnik, and J. M. Albert (2003), Controlled precipitation of radiation belt electrons, *J. Geophys. Res.*, *108*(A5), 1186, doi:10.1029/2002JA009580.
- Iyemori, T., and K. Hayashi (1989), PC 1 micropulsations observed by Magsat in the ionospheric F-region, *J. Geophys. Res.*, *94*(A1), 93–100.
- Jackman, C. H., M. C. Cerniglia, J. E. Nielsen, D. J. Allen, J. M. Zawodny, R. D. McPeters, A. R. Douglass, J. E. Rosenfield, and R. B. Rood (1995), Two-dimensional and three-dimensional model simulations, measurements, and interpretation of the influence of the October 1989 solar proton events on the middle atmosphere, *J. Geophys. Res.*, *100*(D6), 11,641–11,660.
- Kennel, C. F., and H. E. Petschek (1966), Limit on stably trapped particle fluxes, *J. Geophys. Res.*, *71*(1), 1–28.
- Lyons, L., and D. Williams (1984), *Quantitative Aspects of Magnetospheric Physics*, *Geophys. and Astrophys. Monogr.*, D. Reidel, Dordrecht.
- Papadopoulos, K. (2001), Satellite threat due to high altitude nuclear detonation, Presentation at Future of Space: 1st Meeting of Scientific Panel, The Eisenhower Institute, Washington, D. C., 11 December. (Available at <http://www.lightwatcher.com/chemtrails/Papadopoulos-chemtrails.pdf>)
- Parks, G. K. (2004), *Physics of Space Plasmas*, Westview, Oxford, U. K.
- Parmentola, J. (2001), High altitude nuclear detonations (HAND) against low earth orbit satellites (“HALEOS”), Report of the Defense Threat Reduction Agency, Advanced Systems and Concepts Office, Fort Belvoir, Va., April. (Available at <http://www.fas.org/spp/military/program/asat/haleos.pdf>)
- Pu, Z. Y., L. Xie, W. X. Jiao, S. Y. Fu, X. H. Fang, Q. G. Zong, and D. Heynderickx (2005), Drift shell tracing and secular variation of inner zone high energy proton environment in the SAA, *Adv. Space Res.*, *36*, 1973–1978.
- Rodger, C. J., M. A. Cliverd, Th. Ulrich, P. T. Verronen, E. Turunen, and N. R. Thomson (2006), The atmospheric implications of radiation belt remediation, *Ann. Geophys.*, *24*, 2025–2041.
- Schulz, M., and L. J. Lanzerotti (1974), *Particle Diffusion in the Radiation Belts*, Springer-Verlag, Berlin, Germany.
- Selesnick, R. S., M. D. Looper, and R. A. Mewaldt (2007), A theoretical model of the inner proton radiation belt, *Space Weather*, *5*, S04003, doi:10.1029/2006SW000275.
- Steer, I. (2002), Briefing: High-altitude nuclear explosions: Blind, deaf and dumb, *Janes Defense Weekly*, 20–23.
- Steinacker, J., and J. A. Miller (1992), Stochastic gyroresonant electron acceleration in a low beta plasma: I. Interaction with parallel transverse cold plasma waves, *Astrophys. J.*, *393*, 764–781.
- Summers, D., and R. M. Thorne (2003), Relativistic electron pitch-angle scattering by electromagnetic ion cyclotron waves during geomagnetic storms, *J. Geophys. Res.*, *108*(A4), 1143, doi:10.1029/2002JA009489.
- Verronen, P. T., A. Seppala, M. A. Cliverd, C. J. Rodger, E. Kyrola, C. F. Ulrich, and E. Turunen (2005), Diurnal variation of ozone depletion during the October–November 2003 solar proton events, *J. Geophys. Res.*, *110*, A09S32, doi:10.1029/2004JA010932.
- Walt, M. (1996), Source and loss processes for radiation belt particles, in *Radiation Belts: Models and Standards*, edited by J. F. Lemaire, D. Heynderickx, and D. N. Baker, *Geophys. Monogr.* 97, pp. 1–13, AGU, Washington, D. C.

K. Papadopoulos, X. Shao, and A. S. Sharma, Department of Astronomy, University of Maryland, College Park, MD 20742, USA. (dapadop@umd.edu; xshaoup@yahoo.com; xshcn@astro.umd.edu; ssh@astro.umd.edu)